



# SEM & FTIR Analysis of Rice Husk to Assess the Impact of Physiochemical Pretreatment

Latika B\* and DilipKumar S

Department of Microbiology and Bioinformatics, Atal Bihari Vajpayee University, Chhattisgarh, India

## Abstract

Pretreatment is one of the pivotal processes in utilizing lignocellulosic biomass for producing bioethanol. An ecofriendly system only allows mild pretreatment strategies for industrial bioethanol production. The steam explosion pretreatment process is reported to be efficient using rice husk for these procedures with the use of mild acids or bases. In the current work, pretreatment method like steam explosion pretreatment method was used with NaOH and HNO<sub>3</sub> to degrade the complex structures and release the sugars entrapped within lignin. The pretreatment effect on the matrix of husk cell-wall and its constituents are characterized microscopically and spectroscopically by scanning electron microscopy and Fourier Transform Infrared Spectroscopy respectively, in order to comprehend the future possibility of its digestion by cellulase. The crystallinity index of native substrate is very high (0.94 cm<sup>-1</sup>), which reduced significantly to -0.277<sup>-1</sup> and -0.34 cm<sup>-1</sup> when pretreated with 2% HNO<sub>3</sub> and 10% HNO<sub>3</sub> respectively. The steam explosion pretreatment does not support the degradation of the cellulosic fibrillar arrangement, but causes intense re-localization of lignin. The descriptions of scanning electron microscopy were in agreement with the findings of Fourier Transform Infrared Spectroscopy; the ordered structure generally found in native rice husk was missing, suggesting that the structure of the 2% HNO<sub>3</sub> treated rice husk was more amorphous. The fractional removal of hemicelluloses and total removal of wax is the outcome of this research work. Results revealed that steam explosion pretreatment increases the possibility of digestion by enhancing cellulose accessibility through lignin re-localization and a partial elimination of hemicelluloses rather than by cell wall disruption.

**Keywords:** Bioethanol; Rice husk; Steam explosion; FTIR; SEM and crystallinity index

## Introduction

Growing energy demand for industrial processes, heating and transportation is one of the prominent challenges of 21<sup>st</sup> century [1]. Substitute energy sources are being extensively investigated worldwide, as energy has always been in demand due to the advanced technologies and population [2]. Challenges like oil dependency are also compelling nations to extend their research for alternative fuels [3]. Potential gaseous biofuels are now available in the form of biohydrogen that can be generated out of waste in microbial electrolysis cells [4]. Bioethanol is a striking unconventional fuel being bio-based renewable resource. Moreover, it supports the reduction in particulate production being oxygenated [5]. Ethanol displays clean burning distinctiveness as its octane number is high and Reid vapor pressure is less [6].

Chemical, physical or biological modes of pretreatment are well explored methods for producing ethanol from Lignocellulosic Biomass (LB). The pretreatment not only augment the biodigestibility of the lignocelluloses for producing ethanol but also enhance accessibility of the enzymes to the biomass. The complex biodegradable materials get enriched by this process, thereby improving the ethanol yield from wastes [7]. Cellulose (35-50 wt. %, dry basis), hemicelluloses (15%-30%), pectin (2%-5%), and lignin (12%-35%) are the chief constituents of LB. Cellulose and hemicelluloses constitute more than 50% of the entire biomass. Sugars generated out of these components can be converted to ethanol [8]. Pretreatment not only leads to the depolymerizing and solubilizing of hemicelluloses polymers, but also disrupts the matrix of cell wall as well as the association amid carbohydrates and lignin [9]. This ameliorates contact for the saccharifying enzymes and improves mass-transport restriction [8]. Degree of cellulose crystallinity also gets changes momentarily after pretreatment [10].

Alkaline pretreatment employs bases such as NaOH, KOH, NH<sub>4</sub>OH, CaOH for the lignocellulosic biomass pretreatment. This process leads to the ester degradation and degradation of glycosidic side

## OPEN ACCESS

### \*Correspondence:

Latika Bhatia, Department of Microbiology and Bioinformatics, Atal Bihari Vajpayee University, Chhattisgarh, India

Received Date: 11 Sep 2023

Accepted Date: 10 Oct 2023

Published Date: 19 Oct 2023

### Citation:

Latika B, DilipKumar S. SEM & FTIR Analysis of Rice Husk to Assess the Impact of Physiochemical Pretreatment. Arch Food Sci Technol. 2023; 2(1): 1007.

Copyright © 2023 Latika B. This is an open access article distributed under the Creative Commons Attribution License, which permits unrestricted use, distribution, and reproduction in any medium, provided the original work is properly cited.

chains those consequences in structural alteration of lignin, swelling and fractional decrystallization of cellulose and limited solvation of hemicelluloses [11]. NaOH aids in disruption of lignin assembly of the biomass, enhancing the approachability of enzymes to cellulose and hemicelluloses [12]. Acid pretreatment causes disjunction of the stringent configuration of the lignocellulosic biomass. Dilute Nitric Acid (HNO<sub>3</sub>) is the most frequently used acid, which has been commercially employed to pretreat a broad spectrum of biomass [13].

Recently, Chhattisgarh Council of Science and Technology (CGCOST), Chhattisgarh, India, funded project on investigation of Bio-valorization ability of rice husk for bioethanol production has outcome in a steam explosion pretreatment procedure for rice husk that has verified to be efficient at formulating rice husk for enzymatic hydrolysis. Amongst the explored pretreatment methods, the Steam Explosion (SE) materializes one of the main ensuring approaches as it restricts the usage of chemicals frequently to the usage of saturated steam [14]. Steam explosions employs steam under pressure at the temperature ranging from 160°C to 260°C for few minutes to disorganize the structure of lignocellulosic biomass [15].

Microscopic techniques such as Scanning Electron Microscopy (SEM), has lined a pathway headed for an extensive comprehending of the fundamental molecular design of plant cell wall. Various other sophisticated procedures like Fourier Transform Infrared (FTIR) spectroscopy have also contributed in process upgradation [16]. In the current study, SEM explores of the effect of steam explosion pretreatment on rice husk cell wall disorder, composition, ultra-structure and exterior properties were studied in order better to comprehend the possibilities of its future digestion with cellulase. Chemical disintegration into component polymer classes was conceded out for all sample varieties. Qualitative determinations of the structural alterations in rice husk post physiochemical pretreatment were done with the help of FTIR. FTIR is an analytical tool that executes a quick and non-persistent admittance of investigating biomolecules by spawning authentic and unrivaled spectral signatures crop up from diverse endogenic functional groups existing in the biomolecules. FTIR is a reagent-free procedure with minuscule procedure that involves very less sample to figure out the biochemical finger print [17].

Taking all the above facets into contemplation, the intend of the research is to obtain FTIR and SEM profile of native and pulverized rice husk in order to understand its feasibility for further enzymatic digestion. FTIR spectroscopy and SEM were used to achieve the above aim as analytical means for qualitative determination of structural alteration in native and pretreated rice husk after physiochemical pretreatment.

## Materials and Methods

### Raw material and its collection

The substrate used is rice husk and it was collected from nearby rice mill from Bilaspur district (22.05°N 82.09°E/22.09°N 82.15°E) Chhattisgarh, India.

### Processing of lignocellulosic substrates

The collected substrate was dried in a forced air oven at 50.0°C for 24 h and milled in a hammer mill to pass through a 1.30 mm screen. The milled substrate was conserved in sealed plastics bags at 4°C to avoid any potential degradation or spoilage.

## Chemicals

Qualitative analytical reagents were procured from Sigma Aldrich Chemicals Pvt. Ltd., Bangalore. Organic solvents were purchased from Sisco Research Laboratories (SRL) and Qualigens Fine Chemicals, India.

### Rice husk sample preparation for analyses

Diverse pretreatment procedures such as steam explosion at 160°C for 60 min; dilute nitric acid (2% v/v), concentrated nitric acid (10% v/v), sodium hydroxide (2% w/v), sodium hydroxide (10% w/v) with steam explosion at 160°C for about 20 min, were implemented separately for the pretreatment of rice husk. The pretreated husk was collected and filtered in crucibles followed by a wash with distilled water under suction. The remains left behind was thoroughly washed twice with distilled water to eliminate all associated chemicals and were air dried at 40°C for 48 h, after which they were used for FTIR and SEM analysis.

### Fourier-transform infrared spectroscopic analysis

The structural attributes of polysaccharides sample were recorded on a Fourier-transform infrared spectrophotometer (IR Affinity-1, Shimadzu, Japan). The samples were grounded with KBr powder (spectroscopic grade) and then pressed into 1 mm pellet for FTIR measurement in the frequency range 400 cm<sup>-1</sup> to 4000 cm<sup>-1</sup>, with a spectral resolution of 0.5 cm<sup>-1</sup>. The spectra would be achieved with an average of 64 scans. Analysis was executed on both the native and pretreated samples. The baselines of the spectra were regulated and normalized with the IR solution software, and the absorption bands at 1427 cm<sup>-1</sup> and 898 cm<sup>-1</sup> were employed to calculate the crystallinity index [18].

To assure that the surfaces measured were identical to those investigated by microscopy, the samples were not homogenized preceding to spectral analysis. The risk taken when selecting this procedure was that the surface cells of the native rice husk were not representative for the bulk material. In order to check whether this was the case, some untreated material was ground to a fine powder, and FTIR spectra were obtained from the homogenized material. There were insignificant differences found between these spectra and those from the non-homogenized samples.

Spectra were recorded from three different sub-samples per sample type, and all spectra were corrected according to the Standard Normal Variate (SNV) method [19]. The mean spectrum of the three corrected spectra is presented for each sample type.

### Scanning electron microscopy and elemental X-ray analysis

Scanning electron micrographs of untreated and treated rice husks was performed with an EVO MA10 (Carl Zeiss) Japan, operated at 20 kv. The samples were coated gold with a SC7620 manual high resolution sputter coater (Quorum Technologies, Newhaven, UK). The sample powder was sprinkled as a thin layer on an adhesive tape placed on the brass sample holder. Surplus amount of the sample was eliminated by blowing with the air spray. The adhered sample was then layered with gold powder employing the sputtering device.

Characteristic X-rays were detected by Oxford instruments attached with above mention SEM model, and further elemental X-ray analysis was done with the help of EDX software.

## Results

### FTIR spectroscopic analysis

FTIR spectroscopy was employed as an analytical means for qualitative determination of the chemical alterations on the surface of steam explosion pretreated rice husk separately with 2% and 10% each with HNO<sub>3</sub> and NaOH, to accompany and comprehends microscopic explorations. The FTIR spectra of above samples along with their native counterpart are shown in Figure 1.

The cellulose spectrum has three distinctive peaks at wave numbers of 1634 cm<sup>-1</sup>, 1427 cm<sup>-1</sup> and 899 cm<sup>-1</sup>. Small peaks or shoulders were there at wave numbers of 1367 cm<sup>-1</sup>, 1319 cm<sup>-1</sup>, 1337 cm<sup>-1</sup>, 1284 cm<sup>-1</sup>, 1203 cm<sup>-1</sup>, 1161 cm<sup>-1</sup>, 1119 cm<sup>-1</sup>, 1114 cm<sup>-1</sup> and 999 cm<sup>-1</sup>. Similarly, hemicellulose (Xylan) had major peaks at wave numbers of 1646 cm<sup>-1</sup>, 1563 cm<sup>-1</sup>, 1044 cm<sup>-1</sup> and 899 cm<sup>-1</sup> and small peaks or shoulders at wave numbers of 1508 cm<sup>-1</sup>, 1461 cm<sup>-1</sup>, 1420 cm<sup>-1</sup>, 1252 cm<sup>-1</sup>, 1212 cm<sup>-1</sup>, 1164 cm<sup>-1</sup> and 990 cm<sup>-1</sup>. The lignin spectrum demonstrated characteristic peaks at wave number of 1697 cm<sup>-1</sup>, 1603 cm<sup>-1</sup>, 1514 cm<sup>-1</sup> and 837 cm<sup>-1</sup>. A few small peaks were observed at wave numbers of 1457 cm<sup>-1</sup>, 1423 cm<sup>-1</sup>, 1327 cm<sup>-1</sup>, 1281 cm<sup>-1</sup>, 1121 cm<sup>-1</sup> and 1034 cm<sup>-1</sup> [20].

Two interesting features are shown in Figure 1 A2. First it can be seen that the carbonyl band at 1735 cm<sup>-1</sup>, which has been attributed to hemicelluloses is diminished for all pretreated rice husk. This is anticipated as the pretreatment is known to eliminate a huge portion

of hemicelluloses. Second, lignin bands at approximately in 1510 cm<sup>-1</sup> (aromatic ring stretch) are strongly enhanced in 10% NaOH pretreated samples of rice husk compared with that of native one, where these peaks are diminished (Figure 1 A2).

Presences of various bands in FTIR spectrum of native and pretreated rice husk are given in Table 1. The CI of native rice husk is very high (0.94 cm<sup>-1</sup>) while the pretreated substrate with 2% NaOH is 0.01, 10% NaOH is 1.02, 2% HNO<sub>3</sub> is -0.277, 10% HNO<sub>3</sub> is -0.34 cm<sup>-1</sup> (Figure 2). This shows high difference.

### Scanning electron microscopy analysis

Based on the outcomes from FTIR spectroscopy, scanning electron microscopy was employed to assemble information on the consequence of the steam explosion pretreatment on the ultra-structure and potential disorder of the cell wall. SEM technology was employed for morphological studies of both native and modified rice husk, so to achieve visualized imminent.

As it can be seen in Figure 3A, 3B, outer epidermis of rice husk, is well constructed and has a crumpled arrangement. The structure simulates that of an amalgamated material with fibers (silica) properly interspaced in the matrix (cellulose, hemicellulose and lignin). The outer epidermis was extremely uneven and highlighted a linear edged conformation with dazzling dome-like constitutions, due to a more concentrated allotment of silica. However, a prior study pertaining Field-Emission Scanning Electron Microscopy (FE-SEM) and Energy

**Table 1:** Presence of various bands in FTIR spectrum of native and pretreated rice husk.

Absorbance at	Native	2% NaOH	10% NaOH	2% HNO <sub>3</sub>	10% HNO <sub>3</sub>	Inferences
3600-3000	0.15	0.13	0.22	-0.003	0.07	This range comprises bands related to crystalline structure of cellulose. It is related to the valence vibration of H-bonded OH and intramolecular H-bonds
1463	-	-	+	+	+	CH <sub>2</sub> +CH <sub>3</sub> deformation of lignin
1733	+	-	+	-	-	Chemical changes in hemicellulose or lignin
1515	-	-	+	+	+	C=C aromatic skeletal vibration
1300-1000 -1058	-	+	-	-	-	Penetration of chemical in the amorphous region of the biomass and degrading hemicellulases
1606	-	+	-	-	-	Lignin was also degraded by the action of HNO <sub>3</sub> . Hence lignin is not composed of % phenyl And aromatic skeletal vibration
2850	-	-	-	+	+	Both are characteristics of cellulose
2918	-	-	-	+	+	Both are characteristics of cellulose
1164	-	+	-	-	-	peak of pure cellulose 1160-glycosidic linkage
1010	-	+	+	-	-	
CI=1427/898	0.94	0.01	1.02	-0.277	-0.34	
1725	+	-	-	-	-	A simple carbonyl group such as ketone, ester
1545	+	-	-	-	-	C-C=C asymmetric stretching
1630-1660	+	+	-	-	-	Amide C=O stretching
1260	-	+	-	-	-	C-O stretching
900	-	+	-	-	+	anti-symmetric out-of-plane ring stretch of amorphous cellulose; C-O stretching
2840/2835	-	+	--	-	-	H-C-H asymmetric and symmetric stretching
2700-3000	-	-	+	-	-	Refers aliphatic compounds
1300-1600	-	-	+	-	-	Simple hydroxyl compound
15,101,460	-	-	-	+	+	semicircle ring stretching (aromatic lignin)
13,801,540	-	-	-	+	+	C-H symmetric and asymmetric deformation
1600	-	-	+	-	-	C-C=C asymmetric stretching, this band associated with lignin
1650	+	-	+	-	-	Due to C=O stretching
1460/1462	-	+	+	+	+	C-H deformation (methyl and methylene)

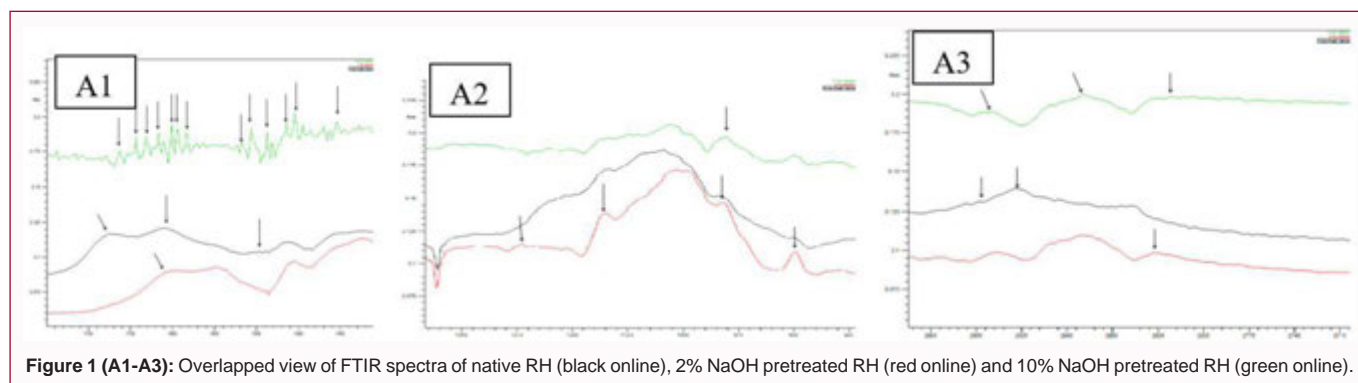


Figure 1 (A1-A3): Overlapped view of FTIR spectra of native RH (black online), 2% NaOH pretreated RH (red online) and 10% NaOH pretreated RH (green online).

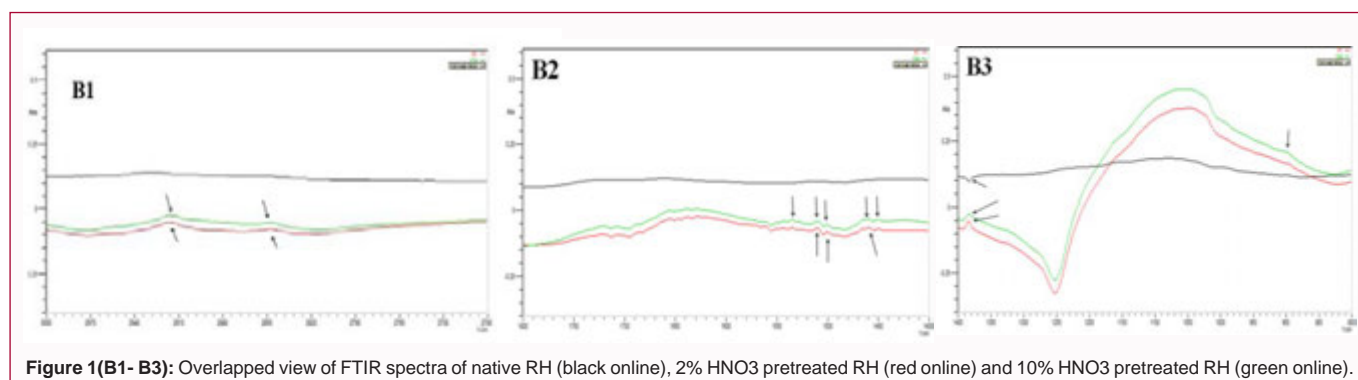


Figure 1 (B1-B3): Overlapped view of FTIR spectra of native RH (black online), 2% HNO<sub>3</sub> pretreated RH (red online) and 10% HNO<sub>3</sub> pretreated RH (green online).

Dispersive X-Ray Micro-Analysis (EDXA) machinery established that silica also emerged in other parts of rice husk with a comparatively low concentration.

The silica is primarily confined to a small area in the rice husk's sturdy interlayer (epidermis) and filling in the spaces sandwiched between the epidermal cells. The concentration of silica was elevated on the exterior surface of the husk and much feeble on the inner face and virtually missing inside the rice husk. Figure 3A, 3B shows the standard spherical platelets of approximately equivalent size (40 lm-50 lm) emerging in equivalent rows.

Primarily, the most perceptible consequence of the steam explosion pretreatment distant from a color transform from golden brown into dark brown is the fractional defibration, or separation of individual fibers and cell types of the rice husk (Figure 3C). As it can be seen in Figure 3C, the exterior structure of the rice husk residues transformed considerably after 2% HNO<sub>3</sub> under steam explosion. Diminution of roughness on the outer surface and particle cracking, suggests weakening of rice husks due to hike in brittleness. Structural disruptions resulted in the improvement of accessibility of the interior parts of the cell wall matrix. Pits and perforations can be seen (Figure 3C).

Post treatment by 2% HNO<sub>3</sub>, the slight film (wax layer) on the exterior part vanished totally, the consistency was unstructured and fragmented, and some holes emerged on the solids surface. This signifies that the sample structure was dislocated by 2% HNO<sub>3</sub> treatment to an immense level. These alterations were valuable for the proficient biodegradability and the employment of rice husk for later cellulase digestibility.

Although the pretreated material is quite varied and holds larger pieces (up to about 1 cm) that are effortlessly identified as husk, a relevant fraction consists of cells that are either wholly or

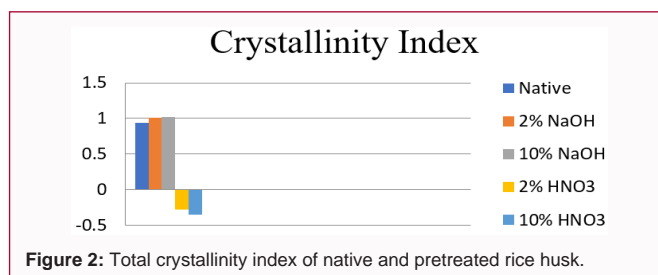


Figure 2: Total crystallinity index of native and pretreated rice husk.

moderately detached from each other. All individual fibers seem to be unbroken despite the steam explosion pretreatment, slightly than being damaged or otherwise dislocated (Figure 3D). Close scrutiny of pretreated fibers reveals the presence of debris covering the surface and deposition of thin layer covering the entire surface (Figure 3A). These fragments could be parts of middle lamellae. As it can be seen in Figure 3D, the exterior micrographs demonstrate domes broken after the treatment step representing that at least part of inorganic fraction (mainly silica) was removed. As it can be seen in Figure 3C, 3D, significant structural variations occurred on the overall or fibrillar organization of the individual fibers that includes perceptible augment of porosity. Treatment with 2% NaOH resulted in absolute elimination of the superficial surface. Samples appeared lighter, constituting chiefly cellulose with lower thermal constancy than the native one (Figure 3A, 3E). As it can be seen in Figure 3E, the native organization of rice husk was almost damaged and the inorganic portion (mainly silica) there as the conical projections on the native rice husks was eliminated. The removal of the outer surface and the disappearance of the inner surface also implicit the removal of the organic part (Figure 3F).

## Discussion

As it can be detected in the Figure 1 A1, 1 A3, the untreated



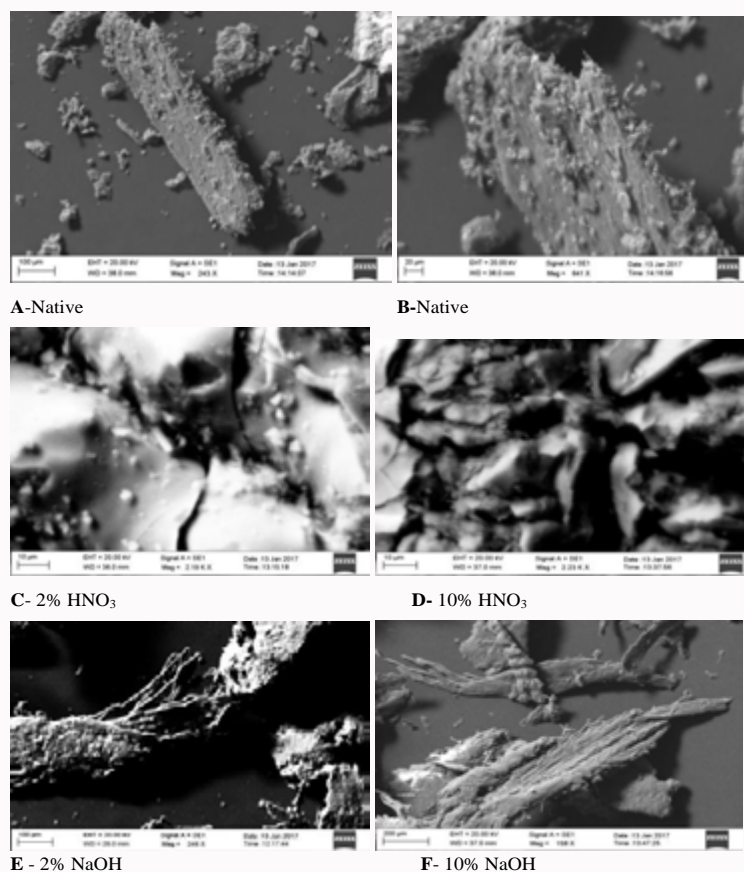


**Figure 3:** (A-F) Scanning Electron Microscopic images of native rice husk and pre-treated (2% & 10% HNO<sub>3</sub>/NaOH) rice husk.

rice husk samples obtained various bands at 1650/1655  $\text{cm}^{-1}$  which revealed a heterogeneity in the absorption intensity, conform either to carboxylates or the absorbed water; therefore, the difference in the absorption intensity probably expresses various cargo of carboxylates, as all samples were dried following the same protocol [21]. While the band at 1545  $\text{cm}^{-1}$  is due to C-C=C asymmetric stretching and band at 1725  $\text{cm}^{-1}$  the compound is apparently a simple carbonyl compound, such as a ketone, an aldehyde, an ester, or a carboxylic acid. The band at 1065  $\text{cm}^{-1}$  anticipate the in-plane C-H bending vibrations of aromatic compounds symbolically arise in this region, and can endure as complex band structures (multiple, distinct bands). They gravitate not to be diagnostic for various compounds because of clash and convergence with other functional group absorptions, including some skeletal (backbone) vibrations. Band at 1200  $\text{cm}^{-1}$  speculate that the compound is likely to be a simple hydroxyl compound because the simple hydrogen-bonded OH absorption of a hydroxy (alcohol) function has a very distinctive shape. The band at 2925  $\text{cm}^{-1}$  anticipates that they are aliphatic compounds [22]. The peak monitored after pretreatment with 2% NaOH were in range 1630  $\text{cm}^{-1}$  to 1690  $\text{cm}^{-1}$  and are due to amide C=O stretching. The carbonyl stretching absorption is one of the robust IR absorptions, and is very useful in structure assurance ([chem.ucla.edu/webspectra](http://chem.ucla.edu/webspectra)). The frequency range between 1200  $\text{cm}^{-1}$  to 1000  $\text{cm}^{-1}$  has a large contribution of hemicelluloses and cellulose with maxima at 1037  $\text{cm}^{-1}$  due to C-O stretching mode and 1164  $\text{cm}^{-1}$  due to the asymmetrical stretching C-O-C [23,24]. Adapa et al. [20], stated that the peak at 1164  $\text{cm}^{-1}$  refers the existence of cellulose while Robert et al. [25], stated the presence of glycosidic linkage. Evident changes were also observed in

the lignin-characteristic bands around 1606  $\text{cm}^{-1}$ , and therefore, it is feasible to affirm that the lignin was also degraded by the action of the 2% NaOH [26]. Adapa et al. [20], also reported the presence of pure lignin and this peak also speaks for the aromatic skeletal vibration [27,28]. The band monitored at 1260  $\text{cm}^{-1}$  is due to the C-O stretching [22]. The peak scrutinized at 2835  $\text{cm}^{-1}$  was due to H-C-H asymmetric & symmetric stretch. Bekiaris et al. [21], stated that the band at 900  $\text{cm}^{-1}$ /898  $\text{cm}^{-1}$  can be authorized to amorphous cellulose while band at 895  $\text{cm}^{-1}$  to  $\beta$ -1-4 linkage [25] and band at 900  $\text{cm}^{-1}$  speak for the anti-symmetric out-of-plane ring stretch of amorphous cellulose [29]. Band at 1000  $\text{cm}^{-1}$  characterize the pure cellulose [20].

The band observed after pretreatment with 10% NaOH was focused around 1600  $\text{cm}^{-1}$  and 1500  $\text{cm}^{-1}$ , usually crop up as a pair of band structures, often with some crumbling. The display and ratio of these band structures is firmly reliant on the position and nature of substituent on the ring [22]. The absorption in 1733  $\text{cm}^{-1}$  is by virtue to a C=O unconjugated stretching of hemicelluloses but also with the allowance of lignin. Absorption around 1733  $\text{cm}^{-1}$  specifies chemical changes in hemicellulose and/or lignin. The absorption around 1463  $\text{cm}^{-1}$  reveals to CH<sub>2</sub> and CH<sub>3</sub> deformation of lignin [26]. Absorption around 1515  $\text{cm}^{-1}$  is linked with C=C aromatic skeletal vibration [27]. The frequency spectrum between 1200  $\text{cm}^{-1}$  to 1000  $\text{cm}^{-1}$  has a large input of hemicelluloses and cellulose with maxima at 1037  $\text{cm}^{-1}$  due to C-O stretching mode [23]. The band observed between 1300  $\text{cm}^{-1}$  to 1600  $\text{cm}^{-1}$  is likely to be simple hydroxy compound. Coates [22] stated that the band between 2700  $\text{cm}^{-1}$  to 3000  $\text{cm}^{-1}$  compound is apparently aliphatic. If the main absorptions are approximately 2935  $\text{cm}^{-1}$  and 2860  $\text{cm}^{-1}$ , and there are also absorptions at 1470  $\text{cm}^{-1}$  and

720  $\text{cm}^{-1}$ , then the compound presumably contains a long linear aliphatic chain.

As it can be seen in the Figure 1 B1 - 1 B3, the band interpretation of pretreated substrates with 2%  $\text{HNO}_3$  observed bands at 1500  $\text{cm}^{-1}$ , 1510  $\text{cm}^{-1}$  is due to aromatic C=C bending (webspectra.ucla.edu) and are associated with lignin [21] while band at 1460  $\text{cm}^{-1}$  is due to N=H bending as well as refers to  $\text{CH}_2$  and  $\text{CH}_3$  deformation of lignin [26]. Absorption around 1515  $\text{cm}^{-1}$  is associated with C=C aromatic skeletal vibration [26]. Band at 1360  $\text{cm}^{-1}$  assumes that a simple hydroxyl compound because the simple hydrogen-bonded OH absorption of a hydroxy (alcohol) function has a very characteristic shape [22]. The small peaks at 2850  $\text{cm}^{-1}$  and 2918  $\text{cm}^{-1}$  originates from  $\text{CH}_2$  and  $\text{CH}_3$  symmetric and asymmetric stretching respectively. Both are characteristic of cellulose [23,30]. The peak at 2920  $\text{cm}^{-1}$  and the shoulder at 2850  $\text{cm}^{-1}$  correspond to aliphatic. Ciolacu et al. [31], observed a variation in this peak from 2900  $\text{cm}^{-1}$  for pure cellulose to 2920  $\text{cm}^{-1}$  for the amorphous cellulose. The band observed after 10%  $\text{HNO}_3$  pretreated substrates were 1380  $\text{cm}^{-1}$ , 1450  $\text{cm}^{-1}$ , 1465  $\text{cm}^{-1}$ , 1500  $\text{cm}^{-1}$ , 1510  $\text{cm}^{-1}$ , 1535  $\text{cm}^{-1}$  and 1580  $\text{cm}^{-1}$  which assumed that it is that a simple hydroxyl compound because the simple hydrogen-bonded OH absorption of a hydroxy (alcohol) function has a very distinctive shape (1300  $\text{cm}^{-1}$ -1600  $\text{cm}^{-1}$ ) [22]. Peak of 1510  $\text{cm}^{-1}$  is due to aromatic C=C bending (webspectra.ucla.edu) and are associated with lignin while 1460  $\text{cm}^{-1}$ , tally to xylans. The band at 900  $\text{cm}^{-1}$ /898  $\text{cm}^{-1}$  can be accredited to amorphous cellulose [21]. The small peaks at 2850  $\text{cm}^{-1}$  and 2918  $\text{cm}^{-1}$  originates from  $\text{CH}_2$  and  $\text{CH}_3$  symmetric and asymmetric stretching respectively. Both are peculiar of cellulose [23,30].

Two interesting features are shown in Figure 1 A2. First it can be seen that the carbonyl band at 1735  $\text{cm}^{-1}$ , which has been attributed to hemicelluloses is diminished for all pretreated rice husk. This is anticipated as the pretreatment is known to eliminate a huge portion of hemicelluloses. Second, lignin bands at approximately in 1510  $\text{cm}^{-1}$  (aromatic ring stretch) are strongly enhanced in 10% NaOH pretreated samples of rice husk compared with that of native one, where these peaks are diminished (Figure 1 A2). One elucidation for this could be a comparative hike in the lignin amount due to the elimination of hemicelluloses. Another basis could be release of lignin and its re-deposition on the surface. The lignin hike is considered too considerable to be only due to the hemicelluloses's exclusion [32].

Reduction in cellulose crystallinity is one of the best strategies engaged to enhance the enzymatic convertibility. Infrared peak ratios describe the comparative amounts of amorphous and crystalline cellulose which differentiates the samples. The crystallinity variation can be studied by accrediting the 1427  $\text{cm}^{-1}$  and 898  $\text{cm}^{-1}$  absorption bands with respective to cellulose I and cellulose II. The absorbance ratio A1427/A898 is acknowledged as Crystallinity Index (CI). Crystallinity of cellulose is one of the crucial factors influencing enzymatic hydrolysis. The lower crystallinity index signifies a higher quantity of amorphous cellulose present in the regenerated cellulose [33].

Silica throughout composition augmented the strength of the rice husk epidermis [34]. Park et al. [35], have revealed from Field-Emission SEM (FE-SEM) and Energy Dispersive X-Ray Micro-Analysis (EDXA) trials, that silica appears to be there all through the outer face of rice husk (domes and their shoulder). The elevated silica substance on outer epidermis offers tenacity and rigidity to the husk.

Figure 3A, 3B shows the standard spherical platelets of approximately equivalent size (40  $\mu\text{m}$ -50  $\mu\text{m}$ ) emerging in equivalent rows. As reported, the majority of the silica prevailed in the superficial epidermal cells, being predominantly cluttered in the dome-formed protuberance [36].

The surface of rice husk residues emerged to be rough and had cracks. The crystallinity index of 2%  $\text{HNO}_3$  treated rice husk is -0.2777. This illustrates that the disintegration and consecutive reclamation of cellulose is dependent on the extent of swelling on the biomass. The disintegration procedure was presage by considerable swelling of the rice husk matrix which could be monitored from the swollen display of the rice husk residue. This rice husk residue illustrated meticulously disordered structure with diminished crystallinity. Rice husk residues from steam explosion pretreatment could be a prospective substrate for bioconversion into value compounds. The disrupted surface configuration of the rice husk residues makes them complimentary for solid state fermentation, where it aids in growth of microorganism by permitting entry of microorganism to the lignocellulosic matrix [33].

The images of SEM were in conformity with the conclusion of FT-IR; the ordered structure frequently present in indigenous lignocellulosic biomass was missing, suggestive of that the structure of the 2%  $\text{HNO}_3$  treated rice husk was more amorphous. This also indirectly specifies that, with 2%  $\text{HNO}_3$  pretreatment, results in reduction of crystallinity of cellulose in comparison to the native rice husk.

As it can be seen in Figure 3C, 3D significant structural variations occurred on the overall or fibrillar organization of the individual fibers that includes perceptible augment of porosity. These variations are considered to be correlated with thermal pretreatments. Holes or cracks were also observed in the fibers.

The complete vanishing of 1732  $\text{cm}^{-1}$  absorbance was revealed in the FTIR spectrum, signifying the absence of hemicelluloses and waxes in this material. Presence of peak at 1606  $\text{cm}^{-1}$  in the FTIR spectra with diminished intensity indicates the existence of un-extracted aromatic compounds [37]. The chief consequences of alkali pretreatment include the reduction in content of lignin and hemicellulose in natural fibers, permitting diffusion of water molecules to the inner layers and cleavage of bonds joining lignin-carbohydrate and hemicelluloses. Along with the removal of hemicelluloses, alkali treatment develops the fiber surface bond distinctiveness and generating rough surface. This type of surface presents better fiber matrix interface bond and an augment in mechanical properties [38].

The light color of the sample indicated that the consequential rice husk after pretreatment is mostly cellulose, as the cementing matter of the lignocellulosic matrix i.e., lignin and hemicelluloses were preferentially degraded. The dark color of raw rice husk is basically due to lignin concentration [34].

The SEM micrographs clearly indicate the significant changes in the morphology of rice husk when the later was treated in alkaline conditions. Both the inner and outer surface of rice husk was affected as an outcome of elimination of silica (inorganic component), hemicellulose and lignin (organic component). The resultant rice husk presented an intense color and a more consistent fiber allocation [34]. The skeletal arrangement is integral with insignificant changes in cellulose crystallinity. Consequently, the pretreatment is effective due to removal of hemicellulose and lignin re-localization. Pretreatment

does not support complete removal of lignin leading to fruitless cellulases adsorption, as lignin enclose the cellulose in the cell-wall matrix, obstructing cellulases from accessing cellulose fibrils.

## Conclusion

Attention was made among global researchers and academicians towards the bioconversion of rice straw and husk for production of bioethanol being source for sustainable and green fuel. Having bestowed in cellulosic biomass with great interest in converting them to bioethanol, rice husk is used as global source for biorefinery purpose. However, due to much recalcitrant than rice straw and producing many fermentation inhibitors efficient treatment processes are to be explored towards healthy saccharification and fermentation.

Morphological alterations of straw by pretreatments were examined via SEM images. Evaluating SEM descriptions of treated and untreated rice husk illustrates remarkable alterations in the surface configuration and porosity. Untreated rice husk had a filled structure covered by a silica layer. However, the silica layer was unwrapped as an outcome of treatment, leading to amplified reachable surface area for the enzyme penetration. Samples treated with HNO<sub>3</sub> and NaOH had a demolished structure and the swelled shape after steam explosion. Hence the SEM examination proved that the rice husk morphology altered significantly post being treated in alkaline conditions. Both the inner and outer surface of rice husk were affected as an outcome of elimination of silica (inorganic component), hemicellulose and lignin (organic component) and the diminution in cellulosic crystallization. This pretreatment ensures the further utility of rice husk to harness left over cellulosic sugar (glucose) by cellulase treatment.

## Funding

Chhattisgarh Council of Science and Technology (CGCOST), Chhattisgarh, India.

## Acknowledgment

We are extremely thankful to Prof. A.D. N. Bajpai, Hon`ble Vice Chancellor, Atal Bihari Vajpayee University for his support and encouragement to pursue this research work. We would like to thank Prof. Rangari, Dr. Sanjay Bharti, Dr. Thareja, Prashant Mishra of Department of Pharmacy, Guru Ghasidas Central University, Bilaspur for their support in doing FTIR in this department. We are thankful to Head of the Department of Physics of Guru Ghasidas Central University, Bilaspur for their support in doing SEM in this department.

## References

- Bhatia L, Sarangi PK, Nanda S. Current advancements in microbial fuel cell technologies. In: Biorefinery of alternative resources: Targeting green fuels and platform chemicals. 2020.
- Show KY, Yan, YG, Le DJ. Biohydrogen production: Status and Perspectives. In: Biofuels: Alternative Feedstocks and Conversion process for the production of liquid and Gaseous Biofuels. 2019;693-713.
- Nanda S, Rana R, Hunter HN, Fang Z, Dalai AK, Kozinski JA. Hydrothermal catalytic processing of waste cooking oil for hydrogen-rich syngas production. Chem Eng Sci. 2019;195:935-45.
- Rivera I, Schröder U, Patil SA. Microbial electrolysis for biohydrogen production: Technical aspects and scale-up experiences. Microb Electrochem Technol. 2019;871-98.
- Yahaya U, Abdullahi UK, Dangmwan DS, Namadi MM. Bioethanol production from eucalyptus camaldulensis wood waste using bacillus subtilis and *Escherichia coli* isolated from soil in Afaka Forest Reserve, Kaduna State Nigeria. Int J Sust Green Energy. 2017;4(2):40.
- Bhatia L, Singh A, Chandel A, Singh OM. Biotechnological Advancements in cellulosic ethanol production. Sustainable Biotechnol Enz Res Renew Energy. 2018.
- Kaur I, Sahni G. Multi-scale structural studies of sequential ionic liquids and alkali pretreated corn stover and sugarcane bagasse. Green Sustain Chem. 2018;8(1):92.
- Bhatia L, Sharma A, Bachetti RA, Chandel AK. Lignocellulose derived functional oligosaccharides: Production, properties and health benefits. Prep Biochem Biotechnol. 2019;49(8):744-58.
- De Jonathan MC, Martini J, Thans SVS, Hommes R, Kabel MA. Characterization of non-degraded oligosaccharides in enzymatically hydrolyzed and fermented, dilute ammonia pretreated corn stover for ethanol production. Biotechnol Biofuels. 2017;10:112.
- Chandel Ak, Garlapati VK, Singh AK, Antunesa FAF, Silvae SS. The path forward for lignocellulose biorefineries: Bottlenecks, solutions, and perspective on commercialization. Bioresource Technol. 2018;264:370-81.
- Zhao W, Ci S. Nanomaterial as electrode materials of microbial electrolysis cell for hydrogen generation. Micro Nano Technol. 2019;213-42.
- Lun LW, Gunny AAn, Kasim FH, Arbain D. Fourier Transform Infrared Spectroscopy (FTIR) analysis of paddy straw pulp treated using deep eutectic solvent. AIP Conf Proc. 2017;1835:020049.
- Nair RB, Kalif M, Ferreira JA, Taherzadeh MJ, Lennartsson PR. Mild-temperature dilute acid pretreatment for integration of first and second generation ethanol processes. Bioresource Technol. 2017;245 (Part A):145-51.
- Alvira P, Tomás-Pejó E, Ballesteros M, Negro MJ. Pretreatment technologies for an efficient bioethanol production process based on enzymatic hydrolysis: A review. Bioresour Technol. 2010;101(13):4851-61.
- Banerjee S, Mudliar S, Sen R, Giri B, Satpute D, Chakrabarti T, et al. Commercializing lignocellulosic bioethanol: Technology bottlenecks and possible remedies. Biofuels Bioprod Bioref. 2010;4(1):77-93.
- Kumar A, Singh D, Chandel AK, Sharma KK. Technological advancements in sustainable production of second generation ethanol development: An appraisal and future directions. In: Sustainable Biofuels Development in India. 2017.
- Kalmodia S, Parameswaran S, Yang W, Barrow CJ, Krishnakumar S. Attenuated total reflectance fourier transform infrared spectroscopy: An analytical technique to understand therapeutic responses at the molecular level. Sci Rep. 2015;5:16649.
- Mirahmadi K, Kabir MM, Jehanipour A, Karimi K, Taherzadeh MJ. Alkaline pretreatment of spruce and birch to improve bioethanol and biogas production. Bioresources. 2010;5(2):928-38.
- Barnes RJ, Dhanoa MS, Lister SJ. Standard normal variate transformation and de-trending of near-infrared diffuse reflectance spectra. Appl Spectrosc. 1989;43(5):772-7.
- Adapa PK, Karunakaran C, Tabil LG, Schoenau GJ. Qualitative and quantitative analysis of lignocellulosic biomass using infrared spectroscopy. Canadian Soc Bioeng. 2009;9:307.
- Bekiaris G, Lindedam J, Peltre C, Decker SR, Turner GB, Magid J, et al. Rapid estimation of sugar release from winter wheat straw during bioethanol production using FTIR-photoacoustic spectroscopy. Biotechnol Biofuels. 2015;8:85.
- Coates J. Interpretation of infrared spectra. A practical approach. In: Encyclopedia Analytical Chemistry. Meyers RA, editor. John Wiley, Sons Ltd, Chichester. 2000;10815.
- Oh SY, Yoo D, Shin Y, Kim HC, Kim HY, Chung YS, et al. Crystalline structure analysis of cellulose treated with sodium hydroxide and carbon

- dioxide by means of X-ray diffraction and FTIR spectroscopy. *Carbohydr Res.* 2005;340(15):2376-91.
24. Colom X, Carrillo F, Nogues F, Garriga P. Structural analysis of photodegraded wood by means of FTIR spectroscopy. *Polym Degradation Stab.* 2003;80(3):543-9.
25. Robert P, Marquis M, Barron C, Guillon F, Saulnier L. FT-IR investigation of cell wall polysaccharides from cereal grains, arabinoxylan infrared assignment. *J Agric Food Chem.* 2005;53(18):7014-8.
26. Bhatia L, Johri S. Fourier transform infrared mapping of peels of *Ananas cosmosus* after acid treatment and its SSF for ethanol production by *Pichia stipitis* NCIM 3498, *Pachysolen tannophilus* MTCC 1077. *Indian J Exp Biol.* 2015;53(12):819-27.
27. Pandey KK. A study of chemical structure of soft and hardwood and wood polymers by FTIR spectroscopy. *J Appl Polym Sci.* 1999;71(12):1969-75.
28. Yu P, Block H, Niu Z, Doiron K. Rapid characterization of molecular chemistry, nutrient make-up and microlocation of internal seed tissue. *J Synchrotron Radiat.* 2007;14(Pt 4):382-90.
29. Stewart D, Wilson HM, Hendra PJ, Morrison IM. Fourier-transform infrared and raman spectroscopic study of biochemical and chemical treatments of oak wood (*Quercus rubra*) and barley (*Hordeum vulgare*) straw. *J Agri Food Chem.* 1995;43(8):2219-25.
30. Chandel AK, Antunes FF, Virgilio A, Maria JB, Rodrigues LN, Singh OV, et al. Ultra-structural mapping of sugarcane bagasse after Oxalic Acid Fiber Expansion (OAFEX) and ethanol production by *Candida shehatae* and *Saccharomyces cerevisiae*. *Biotechnol Biofuels.* 2013;6(1):4.
31. Ciolacu D, Ciolacu F, Popa VI. Amorphous cellulose structure and characterization. *Cell Chem Technol.* 2011;45(1-2):13-21.
32. Kristensen JB, Thygesen LG, Felby C, Jorgensen H, Elder T. Cell-wall structural changes in wheat straw pretreated for bioethanol production. *Biotechnol Biofuels.* 2008;1(1):5.
33. Ang TN, Ngoh GC, Chua ASM, Lee MG. Elucidation of the effect of ionic liquid pretreatment on rice husk via structural analyses. *Biotechnol Biofuels.* 2012;5(1):67.
34. Wang Z, Li J, Barford JP, Hellgrat K, McKay G. A comparison of chemical treatment methods for the preparation of rice husk cellulosic fibers. *IJOEAR.* 2016;2(1):69-77.
35. Park BD, Wi SG, Lee KH, Singh A, Yoon TH, Kim YS. Characterization of anatomical features and silica distribution in Rice Husk using microscopic and microanalytical techniques. *Biomass Bioenergy.* 2003;25(3):319-27.
36. Deshmukh P, Bhatt J, Peshwe D, Pathak S. Determination of silica activity index and XRD, SEM and EDS studies of amorphous SiO<sub>2</sub> extracted from rice Husk Ash. *Trans Indian Inset Met.* 2011;65:63-70.
37. Luduena L, Fasce D, Alvarez VA, Stefani PM. Nanocellulose from rice husk following alkaline treatment to remove silica. *Bioresources.* 2011;6(2):1440-53.
38. Rassiah K, Ali A. A study on mechanical behavior of surface modified rice husk/polypropylene composite using sodium hydroxide. *IJET.* 2016;8:72-82.